Final Progress Report

Work supported by this grant included several projects in theory and in experiment areas. The theoretical work was largely in support of experimental efforts in various laboratories to produce ultracold molecules by laser-induced photoassociation of laser-cooled atoms. We are also working on the theory of Bose-Einstein condensates in double well potentials, using a two-mode model that goes beyond the usual Bose-Hubbard approximation.

Some of our experimental projects exploit the enormously strong forces from multi-frequency light and their possible application to lithography using new cold atom sources [1, 2]. We have demonstrated the deceleration, cooling, collimation, and brightening of a beam of metastable 2^3S helium (He*) using the bichromatic force [1–4]. He* is chosen for these experiments because it offers both infrared and ultraviolet transitions, the necessary high saturation intensities are readily achieved, and its high internal energy can break the bonds of a surface monolayer resist with minimum dosage. We have started atom lithographic nanofabrication experiments with our first samples. In addition, we have done highly successful experiments in atom optics with Rydberg atoms. These are excited in two steps by Stimulated Raman Adiabatic Passage (STIRAP) [5, 6] and then focused by an electrostatic hexapole lens. Neither of these feats have been previously accomplished.

I. MODELING ALKALI DIATOMIC ENERGY LEVEL STRUCTURE TO OPTIMIZE PRODUCTION OF ULTRACOLD MOLECULES

Recently there has been intense effort to produce molecules at temperatures close those achieved for laser-cooled atoms. The possible applications are to coherent chemical processes, low Doppler width studies of collision processes, perhaps a molecular condensate, precision measurements of electron electric dipole moments (with certain polar molecules) and as qubits in a quantum computer. We note in passing that Feshbach resonant states for certain purposes qualify as cold molecules, and have been produced in several laboratories. These are quasi-bound states at the energy of colliding atoms. Though surprisingly stable (with lifetimes up to a second), they are not the electronically and vibrationally ground state molecules that one prefers for many purposes. There has been dramatic progress in electrostatic slowing and trapping of molecular beams, but the minimum temperatures so far have been 25mK [7], rather than tens of μK as one can achieve with laser cooling of atoms. Thus an approach that begins with cold atoms has a starting advantage, if one is willing to consider molecules composed of atoms that can be laser cooled, namely the alkalis and possibly alkaline earths. This technique requires a multitude of lasers to cool and trap the atoms initially, for photoassociation, reexcitation, and detection (see Fig. 1). It also presupposes some knowledge of the structure of the excited state levels, so one objective of our work has been to model the molecular energy level structure and devise the optimum route to ultracold (that is, translationally, rotationally, vibrationally, and electronically cold) ground state molecules.

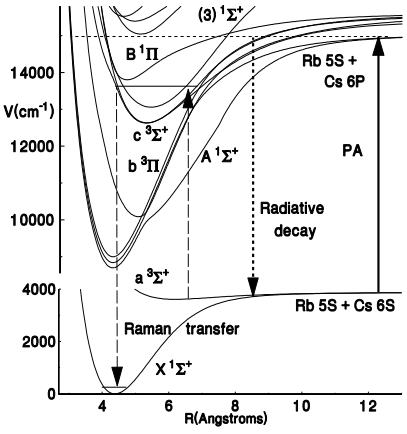

FIG. 1: Scheme for populating the v=0 level of the X state from photoassociation of Rb and Cs atoms, spontaneous radiative decay to levels of the $a^3\Sigma^+$ state, reexcitation to a high level of the $c^3\Sigma^+$ state that is intermixed with $B^1\Pi$, followed by stimulated decay to $v = 0$ of the X state. Here R is the internuclear separation. (From [8, 9])

a. Analysis of data obtained from photoassociation of Rb_2 molecules. There are now a number of schemes for laser photoassociation and stimulated decay to, eventually, hopefully, the lowest vibrational level

REPORT DOCUMENTATION PAGE

Form Approved
OMB NO. 0704-0188

1. AGENCY USE ONLY (Leave Blank)	2. REPORT DATE	3. REPORT TYPE AND DATES COVERED
	27 July 2006	Final Report: 1 Jul 05 to 30 Jun 06

4. TITLE AND SUBTITLE

New Experimental Approaches and Theoretical Modeling Methods for Laser Cooling Atoms and Molecules

5. FUNDING NUMBERS

W911NF-05-1-0407

6. AUTHOR(S)

T. H. Bergeman (PI) and H. J. Metcalf (co-PI)

7. PERFORMING ORGANIZATION NAME(S) AND ADDRESS(ES)

The Research Foundation of SUNY; W5510 Frank Melville Library
Stony Brook University, Stony Brook, NY 11794-3362

8. PERFORMING ORGANIZATION REPORT NUMBER

Award No. 36896

9. SPONSORING / MONITORING AGENCY NAME(S) AND ADDRESS(ES)

U. S. Army Research Office
P.O. Box 12211
Research Triangle Park, NC 27709-2211

10. SPONSORING / MONITORING AGENCY REPORT NUMBER

49093.1-PH

11. SUPPLEMENTARY NOTES

The views, opinions and/or findings contained in this report are those of the author(s) and should not be construed as an official Department of the Army position, policy or decision, unless so designated by other documentation.

12 a. DISTRIBUTION / AVAILABILITY STATEMENT

Approved for public release; distribution unlimited.

12 b. DISTRIBUTION CODE

13. ABSTRACT (Maximum 200 words)

The first part of this project involved continued development of theoretical models of diatomic molecular electronic level structure for application to the production of ultracold diatomic molecules via photoassociation. Recently, there has been considerable interest in producing molecules at the temperatures achieved for laser-cooled atoms, for applications to "coherent chemistry," studies of molecule-atom and molecule-molecule interactions, Bose condensates of molecules and for quantum computing. It is advantageous to produce cold molecules from laser-cooled atoms, but this requires an accurate model of the energy level structure near the dissociation limit for excited atoms, and for other intermediate states. With this in mind, we have modeled experimental photoassociation data from Rb2, spectroscopic data on the lowest excited states of Na2, and hyperfine structure of the lowest triplet state of Cs2.

The second part involved continued development of experimental techniques for intense atomic beam collimation using a bichromatic laser field. We solved the equations for evolution of atoms in such a laser field, expressed the results in the form of trajectories on the Bloch sphere for a two-level atoms, and then used these results to design and perform efficient atomic beam deflection experiments. At the same time, we are developing methods to use these highly collimated beams of metastable helium atoms for precision lithography, using sensitized surfaces.

14. SUBJECT TERMS

Ultracold molecules, photoassociation of atoms, bichromatic laser cooling of atoms, atomic nano-lithography

15. NUMBER OF PAGES

14

16. PRICE CODE

17. SECURITY CLASSIFICATION OR REPORT	18. SECURITY CLASSIFICATION ON THIS PAGE	19. SECURITY CLASSIFICATION OF ABSTRACT	20. LIMITATION OF ABSTRACT
UNCLASSIFIED	**UNCLASSIFIED**	**UNCLASSIFIED**	**UL**

NSN 7540-01-280-5500

Standard Form 298 (Rev.2-89)
Prescribed by ANSI Std. 239-18
298-102

Enclosure 1

of the ground electronic state. This has been successfully demonstrated with work on K_2 [10] and on RbCs molecules, in work in which we collaborated [9], and which is illustrated in Fig. 1. Other approaches have been developed for Rb_2, as discussed in a recent thesis [11]. In each case, the first step is photoassociation of two cold atoms into slightly bound states below the lowest atomic P state. For this reason, it is important to know the energies and properties of these states. At the University of Connecticut, through efforts of a succession of two or three graduate students, excellent data was obtained on excitation of pairs of ^{85}Rb atoms to states below Rb 4S+5P$_{1/2}$, up to binding energies of approximately 80 cm^{-1}. There were three series of resonances, to states of $0_u^+, 0_g^-$, and 1_g symmetry. The first of these connect with electric dipole transitions to the $X^1\Sigma_g^+$ ground state, and the second to levels of the $a^3\Sigma_u^+$ state, which also dissociates to two 5S atoms. The 0_u^+ series was thus a logical starting point for our work. The observed energies for this series indicated a definite perturbation, and of course the perturbing state is the 0_u^+ state that dissociates to the next atomic limit, namely 5S+5P$_{3/2}$. Since the data obtained at U. Conn. for levels below this limit were not of comparable quality, we managed to obtain raw spectral data used for an earlier publication by the D. Heinzen group at the University of Texas in Austin [12].

The paper we wrote on the 0_u^+ states of Rb_2 tending to the 5S + 5P$_{1/2}$ and 5S+5P$_{3/2}$ limits has been accepted for publication in a special issue of the Journal of Physics B on cold molecule formation, scheduled to appear in September, 2006 [13]. It is based on the data from U. Conn. and U. Texas mentioned above, and on *ab initio* calculations of Rb_2 potential curves by S. Lunelle [14]. The energy range of the data, and the potential curves near the 5S+5P limit, are shown in Fig. 2. Since no spin-orbit functions for Rb_2 were available at the time, we used spin-orbit functions calculated by M. R. Manaa for K_2 for our earlier study [15] of this species, but scaled by the ratio of atomic spin-orbit splittings. In addition, parameters for the long-range parts of the two 0_u^+ potentials were taken primarily from a recent study of the pure long range 0_g^- state that dissociates to the 5S+5P$_{3/2}$ limit [16]. The potentials, the spin-orbit functions and the long range parameters were adjusted to achieve an optimized fit to the data. It was established that when the coupling between the two 0_u^+ states was taken into account, the C_3 dispersion coefficient was in fact in close agreement with the value obtained from the 0_g^- state [16], whereas the analysis of the P$_{3/2}$ 0_u^+ data reported earlier [12] yielded a C_3 value differing from the later long-range value by 20 times the quoted error. It was also satisfying, as shown in Fig. 3, that our model calculations reproduced the nearly periodic variation of $B(v)$ values below the P$_{1/2}$ limit due to coupling between the two series. This may be useful in future experiments as it suggests a means to redistribute population from larger to smaller internuclear distances, since states with larger $B(v)$ values are more tightly bound.

We intend to proceed with an analysis of data on the 0_g^- states, and, after working out the hyperfine structure effects, also on the 1_g states.

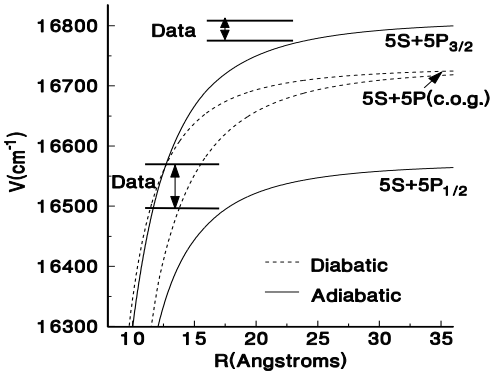

FIG. 2: Rb_2 0_u^+ potentials near the 5S+5P atomic limit, showing regions for which data were available.

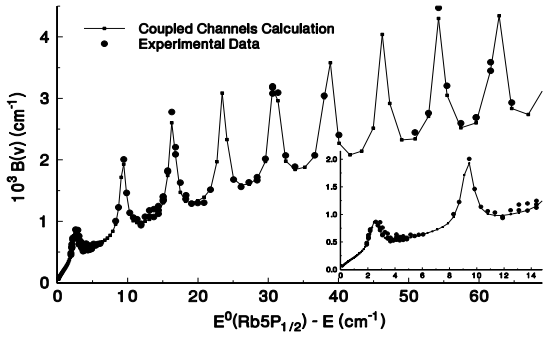

FIG. 3: Results of a fit to rotational parameters, $B(v)$, of the $Rb_2 0_u^+$ series, below the Rb(5S)+Rb(5P$_{1/2}$) threshold. The peaks in $B(v)$ correspond to levels of the 0_u^+ series that dissociate to the Rb(5P$_{3/2}$) threshold.

b. Analysis of spectroscopic data on the Na_2 A and b states. (Numerous collaborators who have

provided experimental data are listed as co-authors of two DAMOP abstracts [17, 18].) One motivation for this work is that the structure of these Na_2 states is simpler due to smaller-orbit perturbations than analogous states of RbCs or Rb_2, and more data are available. Therefore Na_2 spectra have provided useful tests for methods to model the long range and intermediate range potentials, and also tests for numerical techniques. Another motivation is that our spectroscopist collaborators (Li Li and A. M. Lyyra) need accurate estimates of term values of Na_2 levels that have a high degree of singlet-triplet mixing that can be used as "doorway" states to reach higher triplet states from the singlet ground state. In addition to data already compiled by Li and Lyyra, we collected unpublished data from laboratories in Lyon, Toulouse, and MIT, together with published and unpublished data from about 20 sources. Unfortunately, some valuable raw spectroscopic data acquired by P. Kusch and M. Hessel had been tossed out by P. Kusch shortly before his death, and only fitted parameters, with little information on perturbation effects, had been published. Amanda Ross of Lyon proceeded to obtain a comprehensive absorption spectrum that was of almost comparable quality. Not to be outdone, A. M. Lyyra and her student, Peng Qi, have in the past year measured some 17,000 lines by polarization labeled spectroscopy, with sub-Doppler linewidths of about 250 MHz. An overview of the data available, and the relevant potential curves, are shown in Figs. 4 and 5. The assignment of lines and fits to molecular parameters is now nearly complete and has yielded an rms residual of about 300 MHz. A paper will be submitted for publication in the near future.

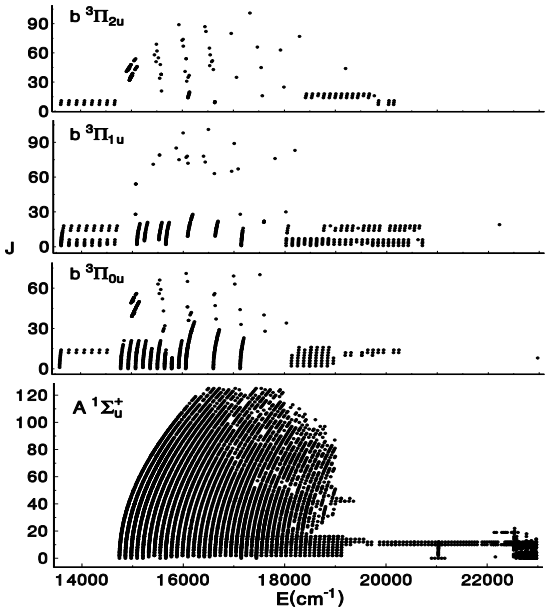

FIG. 4: A summary of the data used in the study of the Na_2 A and b states.

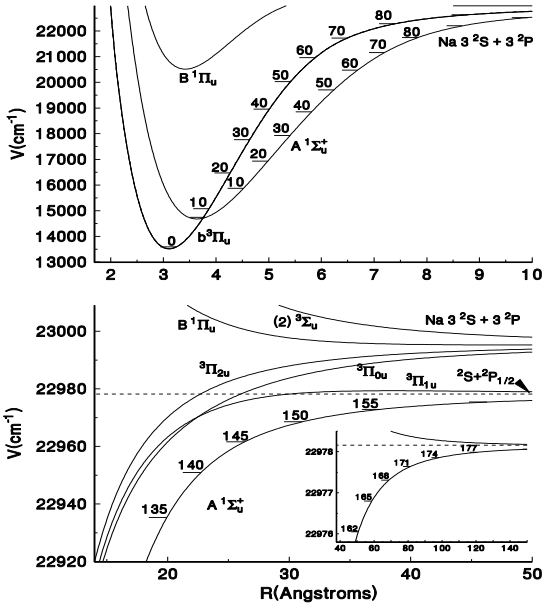

FIG. 5: Potential plots for the A and b states of Na_2.

c. Transformation from atomic to molecular hyperfine structure. In [19], we wrote out explicitly a transformation from a basis of atomic states, known as Hund's case (e), to a case (a) molecular representation for the fine structure (spin-orbit effects). An analogous transformation from atomic to molecular hyperfine structure is needed to assign hyperfine and rotational quantum numbers for photoassociation resonances. $\Omega = 0$ states (with zero electron spin plus orbital angular momentum along the internuclear axis) have negligible hyperfine structure, but $|\Omega|$=1 and 2 levels have complicated hyperfine structure that has eluded analysis in the heavier alkali dimers. For states near the dissociation limit, hyperfine structure dominates rotational structure, so this analysis is needed in order to characterize the states of interest. It may be that photoassociation to some of these levels might lead to more efficient transfer to lower states of interest.

It is intriguing that for Na_2, for example, the Fermi-contact parameters for several molecular electronic states and for many vibrational levels of the $b^3\Sigma_u$ state appear to be roughly the same fraction of the atomic values. This suggests that the dependence on internuclear separation is not critical, and that the above transformation from the free atom case to molecular case a states might be useful at least as an

initial estimate for interpreting molecular hyperfine structure of even deeply bound states. Furthermore, understanding this structure in the ground states is clearly essential for understanding hyperfine structure in excited states since the relative intensities will depend on the nature of the initial ground state.

The angular momentum algebra has been worked out to some extent [20, 21], but we find that the available discussions are incomplete or inadequate for our purposes. During the period of this grant, our work in this area has been devoted to modeling the hyperfine structure of the $a^3\Sigma_u^+$ state of Cs_2, in connection with experiments in Prof. DeMille's laboratory at Yale, reported in the Ph.D. Thesis of S. Sainis. (These experiments were designed to prepare the way to precise measurements of energy differences between levels in the shallow a state potential and levels in the deeper X state as a measure of the ratio of the electron to proton mass and eventually the possible time-dependence thereof.) We have evaluated explicitly the case e to case a transformation for coupled Cs_2 X and a state levels:

$$\langle (f_a, f_b) f, \ell, F | S, I, \Sigma, \iota, parity \rangle. \tag{1}$$

In this expression, the quantities on the left are Hund's case e quantities that apply to the limit of large internuclear separation: $f_i = S_i + I_i$ is the sum of electron spin and nuclear spin for atom i, f is the vectorial sum of f_a and f_b, and ℓ is the nuclear rotation number. The quantities on the right are Hund's case a quantities that refer to the molecular states: S is the total eletron spin, I the total nuclear spin, Σ and ι are the projections of these quantities along the internuclear axis. Elements of the transformation given above involve Clebsch-Gordan factors and nine-J symbols and will not be given explicitly here. The Hamiltonian contains the Born-Oppenheimer potentials and second-order spin-orbit effects which are both defined in case a, while nuclear hyperfine structure and nuclear rotation are defined in case e. The above transformation makes it possible to express the Hamiltonian in either basis.

From calculations as above, we find a rich substructure that has not been systematically explored. Namely, in addition to the usual vibration (v), rotation (here customarily denoted ℓ) and electron spin (S) quantum numbers, there is the total nuclear spin quantum number, I, the vectorial sum $\vec{f} = \vec{S} + \vec{I}$, and then the total angular momentum, $\vec{F} = \vec{f} + \vec{I}$. For two nuclei with spin of 7/2, as for Cs atoms, $I = 0$ ...7, and hence $f = 0...8$. Then for every $F \geq 8$, there are 72 possible case a or case e basis states (apart from the various possible orientations in space). The result is the structure shown in Fig. 6, which shows rotational energies, singlet-triplet splitting, and hyperfine structure for the triplet state, which produces levels that deviate to higher and lower energies. A few experimental data points are also shown in this figure. On top of this, when the spin-spin or second-order spin-orbit effect is not negligible, there are small splittings for different values of F for the same S, ℓ and f. To represent this in Fig. 7, we plot energies as a function of $\ell + f/10 + F/100$. We are presently attempting to extract the magnitude of the second-order spin-orbit effects in each vibrational level from the data.

This work has been in collaboration with D. DeMille and S. Sainis at Yale and with E. Tiesinga of NIST. The detailed calculations have been performed at Stony Brook. A report is in preparation.

II. THE GROSS-PITAEVSKII EQUATION FOR COLD ATOMS IN A DOUBLE WELL POTENTIAL

The graduate student working in this area is supported by NSF, but ARO funds have been used for travel and to purchase a computer. The 14-page paper we published in Physical Review A [22] presented a more rigorous solution for the oscillations of a condensate in a double well potential than previously available for the condition of zero temperature. By using a linear combination of symmetric and antisymmetric functions, we were able to express effects such as the effective change in size of the wavefunction due to interparticle repulsion, as the number of particles in each well varies. This allowed the theory to be carried to larger atom-atom interactions and made it applicable to recent experiments in Heidelberg [23], which were actually the first experimental results for this geometry. Figure 8 compares our results ("improved two-mode model" = ITM) for the oscillation frequency under conditions of the Heidelberg experiments, with results currently prevailing theory [24, 25] ("standard two-mode model" = STM), with a full time-dependent Gross-Pitaevskii equation solution, and with experiment. It is clear that the strong interactions present in the experiment are modeled best by our approach. As Figure 9 shows, the STM yields small amplitude oscillations about the unbalanced configuration, rather than oscillations from one side to the other, as observed, and as calculated by the ITM.

During our visit to Heidelberg in March, we discussed prospects for future development of the theoretical

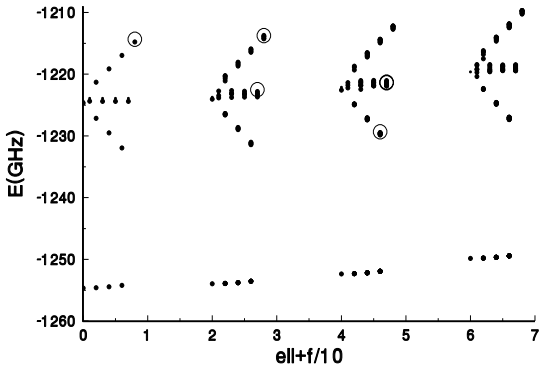

FIG. 6: Hyperfine structure of a Cs_2 $a^3\Sigma_u^+$ level (top) and a nearby $X^1\Sigma_u^+$ level, which does not have appreciable hyperfine splittings. Large open circles are experimental data. The energy scale is relative to the dissociation limit, ell = ℓ is the end-over-end nuclear rotation quantum number, and f is the vectorial sum both of electron spin and nuclear rotation and of the two atomic spin angular momenta, f_a and f_b.

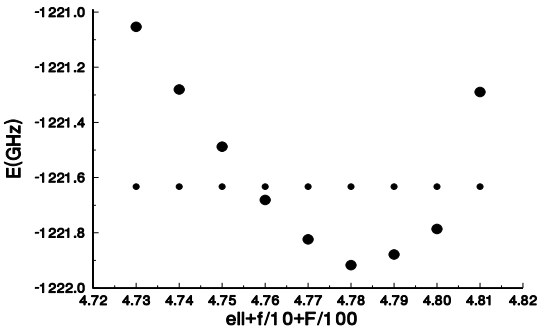

FIG. 7: Detailed structure of an $a^3\Sigma_u^+$ level with $\ell = 4, f = 7$, showing additional splittings as a function of F, the total angular momentum, when the second-order spin-orbit interaction is added to the Hamiltonian.

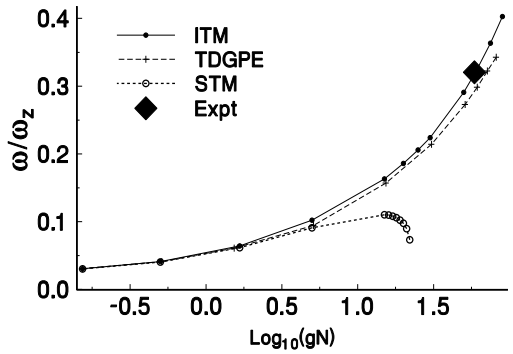

FIG. 8: The solid line gives numerical solutions of the 3d time-dependent Gross-Pitaevskii equation (TDGPE), the dot-dashed and dotted lines are results from the improved (ITM) and standard (STM) two-mode models, respectively, and the diamond represents the experimental frequency observed by [23]. gN denotes the interaction strength times the atom number. The standard model curve terminates due to the onset of self-trapping oscillations, as shown in the next figure.

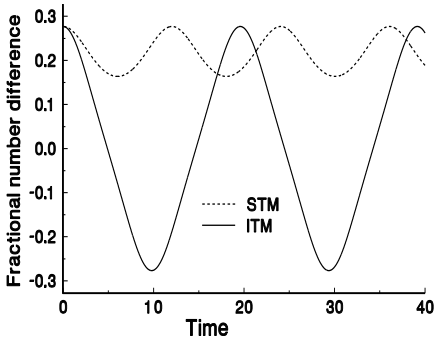

FIG. 9: Time evolution (in units of ω_z^{-1}) of the fractional number difference for conditions of the experiments of Albiez et al. [23], using appropriate parameters for the improved (standard) two-mode model, shown by solid (dashed) line. The STM results show small oscillations within one well, while ITM results show tunneling oscillations as actually observed in the experiments.

and experimental work. Recent experiments have demonstrated damping effects due to thermal atoms, and we have developed theoretical models for these effects. In particular, we have derived expressions for damping of oscillations in the "self-trapping" regime, for which the atom ensemble, in the absence of damping, remains highly unbalanced. There can be damping either for oscillations about this unbalanced configuration, and also decay to a fully balanced configuration, depending on conditions. One important unresolved question is whether quasi-particle sums for thermal atoms can be consistently formulated for the double well situation

when the "condensate" has a two-component nature as mentioned above.

III. STRONG OPTICAL FORCES BY ADIABATIC RAPID PASSAGE

We have observed huge optical forces caused by multiple repetitions of adiabatic rapid passage (ARP) sweeps with frequency-swept, counterpropagating light beams. When the repetition rate of the ARP sweeps, $\omega_s/2\pi$, satisfies $\omega_s \gg \gamma$, the atoms coherently exchange $\pm 2\hbar k$ momentum with the light beams in a time $2\pi/\omega_s \ll \tau \equiv 1/\gamma$, the excited state lifetime [4]. This optical force $F_{ARP} = \hbar k \omega_s/2\pi$ (halved to account for spontaneous emission) is both dissipative and much larger than the maximum value of the ordinary radiative force, $F_{rad}^{max} \equiv \hbar k \gamma/2$.

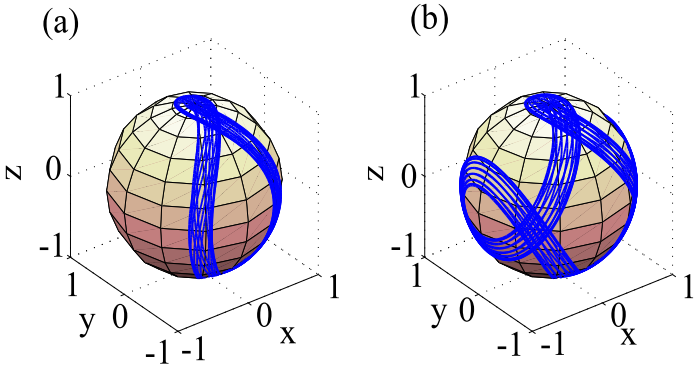

Fig. 10: Unanticipated confined orbits on the Bloch sphere.

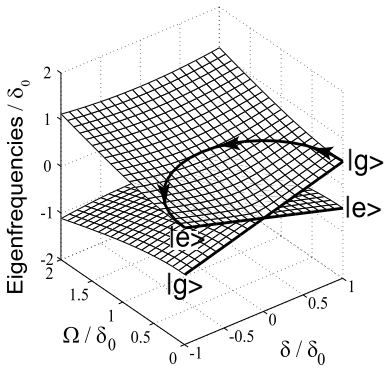

Fig. 11: Dressed state energy surfaces.

We have done numerical studies of adiabatic rapid passage in light that is both frequency and amplitude modulated in the form of chirped pulses, and we found unanticipated confinement of orbits such as those shown in Fig. 10 [26]. We have described this behavior in terms of a periodic Hamiltonian, and obtained a result similar to the Bloch theorem, but in the time domain. This led to further numerical studies, and a quantitative description of the behavior of an atom under multiply repetitive sweeps.

The chirped light pulses drive the atom-laser system up a ladder of dressed state energy sheets on sequential trajectories, thereby decreasing the atomic kinetic energy. One such step is shown by the heavy arrow on the dressed state energy surface of Fig. 11. Nonadiabatic transitions between the energy surfaces must be avoided for this process to be effective. We have calculated the nonadiabatic transition probability for various chirped light pulses numerically and the results relevant to our measurements are shown in Fig. 12. Here the lowest numbers mean the lowest probability for such undesirable transitions. Thus the dark red (in color) regions of parameter space indicate the regions where the ARP force is expected to be the strongest. We have also compared the results with other models and the results are favorable. In addition, an analytical approximation of the nonadiabatic transition probability has been found, and it compares well with the numerical results.

We have developed fiber-based electro-optical systems that can produce the desired chirped pulses in a controlled way with the flexibility to choose the parameters. These resulting laser beams have been applied transversely to our He* atomic beam, and we have inferred the ARP force from the center of the transverse velocity distribution of the deflected atoms. A plot of these measurements over a region of parameter space similar to that of Fig. 12 is shown in Fig. 13. The qualitative comparison of these two figures is clearly excellent.

In developing instruments for such experiments on the $2^3S_1 \rightarrow 2^3P_2$ transition at $\lambda = 1083$ nm in He*, we exploit recent developments in the optical communications industry. We use commercial phase and intensity modulators of the proton-exchanged $LiNbO_3$ waveguide type having V_π as low as 6 V and thus require relatively low rf power for the modulation. Synchronized driving of the two modulators can produce the necessary multiple ARP sequences of 3 ns chirped pulses that span up to a few GHz, as needed for the experiment [2].

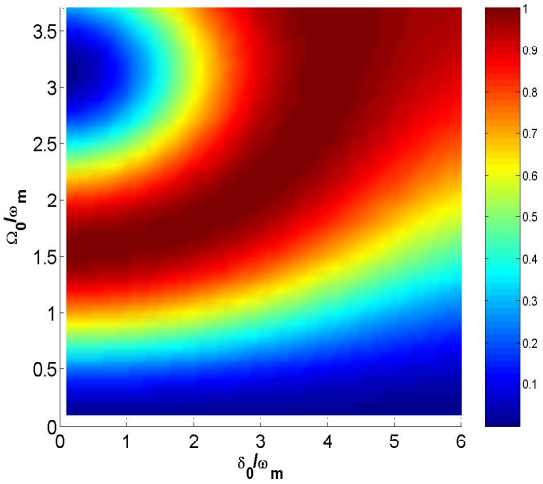

Fig. 12: Map of the regions of various non-adiabatic transitions.

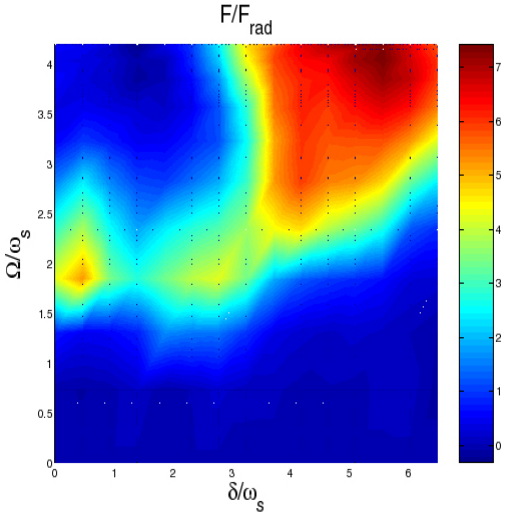

Fig. 13: Contour map of the ARP force inferred from the deflected atomic beam. (The color rendition shows much more similarity to Fig. 12 than the monochrome.)

IV. OUR INITIAL STEPS IN LITHOGRAPHY

We have already made our first attempts at microstructure fabrication, although we are nowhere near the nanostructure scale we are anticipating. Our initial goals were to develop the techniques of coating the substrates, applying the resist layer, experimenting with exposure time in the He* beam, and learning the development and etching process. To do this we gutted and completely revamped one of our 75 m^2 labs, bought and installed a modest AFM and a soft-wall clean room for it, and trained several of the students in its use. We also installed safety and environmental equipment for the chemical processes involved that involve certain less-than-pleasant materials (although nothing is dangerous or highly toxic). Finally, we installed a fume hood inside the clean room, and have assured that it is well-equipped with safety shields and glasses, as well as emergency treatment capability.

We have used our high-brightness He* beam to make our first samples using a large-scale physical mask (12.5 μm pitch metal grid) in place of the wavelength-scale optical patterning mask we anticipate soon. We have used the AFM to measure these first microstructures (Fig. 14). The exposure time of Fig. 14 is shorter than those of earlier experiments and others, but what's important here is that there is no focusing of the atoms, only masking by the grid. With optical patterning that can focus the atoms, features having a spatial duty cycle of 1/10 ($\Rightarrow$ feature size = $\lambda/20$ = 50 nm) can be exposed in 2 minutes, perhaps less.

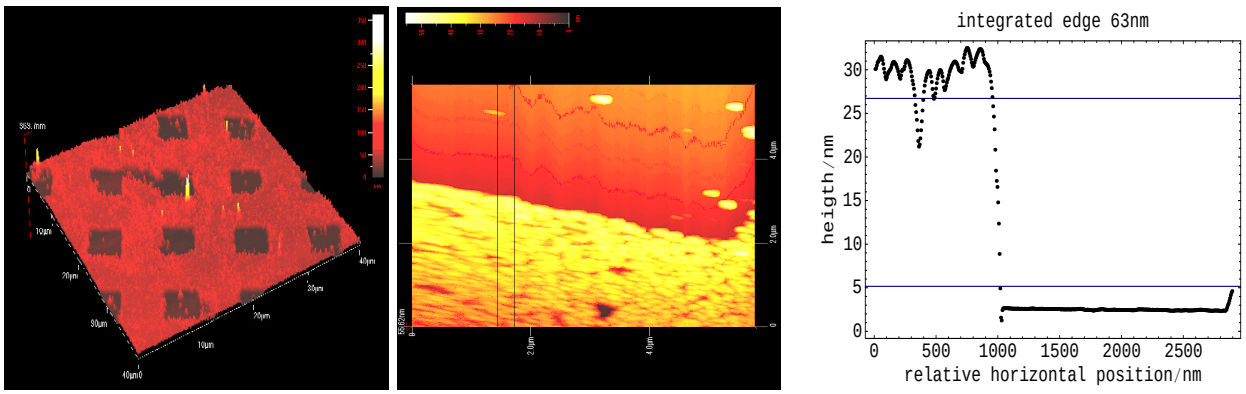

Figure 14: Our first attempts at lithography. The left frame is an overall, large-scale view of the etched image of the grid we use as a mask (the squares are 12.5 μm on a side) exposed to our He* beam for only 20 minutes, the middle frame shows a closeup of one corner of a square hole, and the right frame is the AFM trace over that part of the edge indicated in the center frame. It's clear that even these first primitive structures have the capability of ∼60 nm resolution, and we expect to do considerably better than this.

V. RYDBERG ATOM OPTICS

Although the use of electrostatic forces on atoms is not a new idea, there has not been much success in its implementation [27, 28]. Part of the reason is undoubtedly the limited efficiency of Rydberg state population. In our setup, an atomic beam crosses first one laser beam and then another (both at 90°), and the two-step excitation has a very high efficiency when the atoms encounter the sequence of "light pulses" in the order that corresponds to Stimulated Raman Adiabatic Passage (STIRAP) [5, 6]. The atomic population is coherently driven from the metastable 2^3S state to the ns or nd states using light at $\lambda = 389$ nm and 795 nm that couples through the 3^3P state without ever populating it. It is nearly 100% efficient and is also very tolerant of experimental conditions such as intensity and frequency fluctuations, Doppler shifts, etc.

We excite He atoms in a thermal beam from the metastable 2^3S_1 state (He*) to principal quantum numbers n in the mid-20's. As shown in Fig. 15, this requires light at wavelengths $\lambda = 389$ nm and $\lambda \sim 795$ nm. In our experiment, atoms in an atomic beam cross the laser beams at 90^0 to minimize Doppler shifts and they counterpropagate both to partially cancel residual Doppler shifts, and to minimize the velocity change from recoil. In this way the atoms encounter pulsed light but the production of Rydberg atoms is cw, not pulsed.

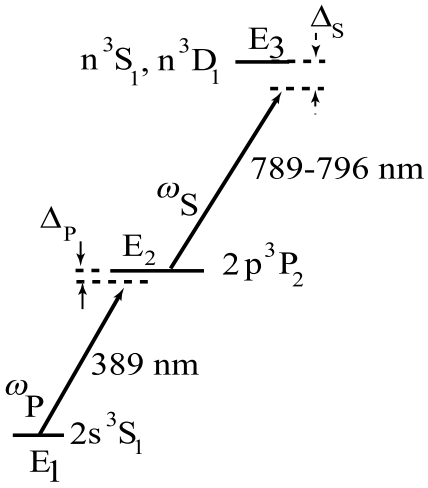

Figure 15. The level scheme for excitation of He* to Rydberg states. The detunings are indicated for the description of the Autler-Townes experiments.

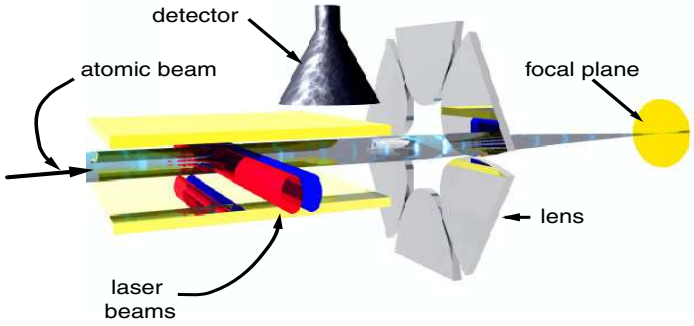

FIG. 16: The experimental arrangement shows the atomic beam passing between the Stark tuning plates where it are crossed by the two laser beams. The intensities and sizes of both nearly-Gaussian laser beams are adjusted to match the optimum conditions for STIRAP for atoms at the mean velocity of our beam, 1200 m/s. The field of only a few V/cm separates the Stark components sufficiently for our lasers to resolve them readily. The Rydberg atoms are then focussed by the hexapole lens to an image plane 1.8 m downstream. Figure not to scale.

Because of the high spectral resolution of the excitation process, our setup can provide a cw high flux source of atoms in specific Rydberg and Stark states for a broad range of experiments, such as focusing He* in an inhomogeneous dc electric field. Such electrostatic focusing can be applied to any atom or molecule that can be put into Rydberg states.

The two laser beams crossing the atomic beam in Fig. 16 can be shifted in space to overlap or to be traversed in normal or in the counter-intuitive order. The intensities and sizes of both nearly-Gaussian beams are chosen to match the optimum conditions for STIRAP for atoms travelling at the mean velocity of our beam of 1200 m/s. Excitation occurs between oppositely charged plates that produce a field of a few V/cm, and this separates the Stark components sufficiently for our laser resolution to resolve them readily.

Because Rydberg atoms display a strong electric dipole moment, we have built an electrostatic hexapole lens and mounted it downstream of the field plates (see Fig. 16). Figure 18 shows the result of the focusing. The beam spot size is about 1 mm, considerably larger than we anticipate for the limiting size. We believe

this large size arises because the incident atomic beam does not emanate from a point and thus constitutes a diffuse source for the lens.

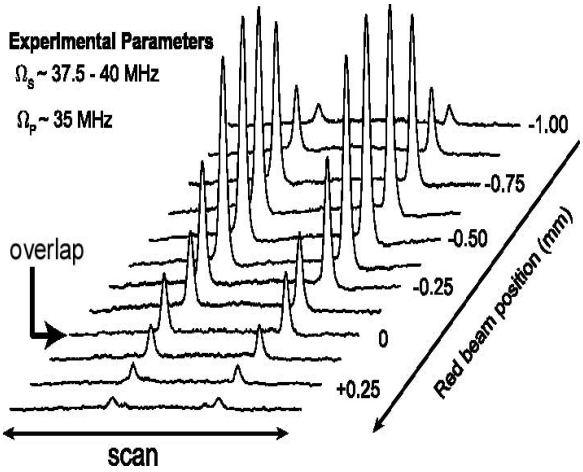

FIG. 17: Each trace shows the result of up/down sweeps of the small dc electrostatic field used to tune the Rydberg state into two-step resonance with the fixed-frequency of the blue and red lasers. The position of these beams along the atomic beam, and thus the order in which they're encountered, varies from -1 mm (red first) to +0.25 mm (blue first). There is a clear and very large enhancement of Rydberg state production in the STIRAP ordering near -0.62 mm.

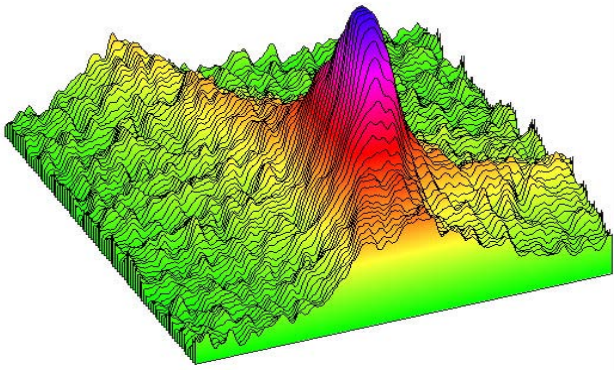

FIG. 18: The result of the focusing for $n = 25$. (The image is produced by an MCP and phosphor screen as in the BF experiments.) The original beam spot is mechanically collimated to be ∼10 mm diameter and this focused spot is 1 mm diam. The major contribution to the 1 mm size is residual transverse motion of the atoms: we are imaging a diffuse source of atoms. We plan to implement ordinary Doppler collimation that effectively puts this source at ∞. We anticipate a sub-micron spot size with nearly all the atoms in the focus. This should enable fast, repetitive writing on a lithographic substrate by applying computer-controlled small signals to the individually addressable lens elements.

Our hexapole electrostatic lens was downstream of the field plates and detector (see Fig. 16), and "optical" axis of the lens was parallel to the atomic beam and through the excitation region. Turning it on did not affect the efficiency or spectral width of the Rydberg excitation. This width was determined by scanning the electric field or the red laser frequency. The lens parameters were chosen to focus states with n in the mid-twenties at voltages ∼100 V. The lens was made using a computerized milling machine and its electrodes' shape was determined with a precision of 10 μm.

Our two step excitation lends itself to the Autler-Townes splitting of the intermediate state [29]. In our case, when the two laser beams overlap, the $\lambda = 389$ nm light produces a splitting of the dressed pair of levels containing the 3^3P state, and the $\lambda = 795$ nm light probes this splitting. Figure 19 shows a typical signal of the Rydberg state production vs. red light frequency, and Fig. 20 shows how the splitting between the peaks depends on the square root of the light intensity. We have measured this and it agrees with our model calculations.

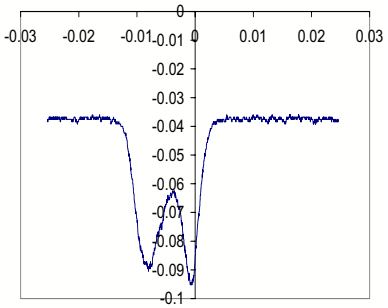

FIG. 19: This shows a typical signal of Rydberg state population vs. frequency of the $\lambda = 795$ nm light in the presence of the $\lambda = 389$ light.

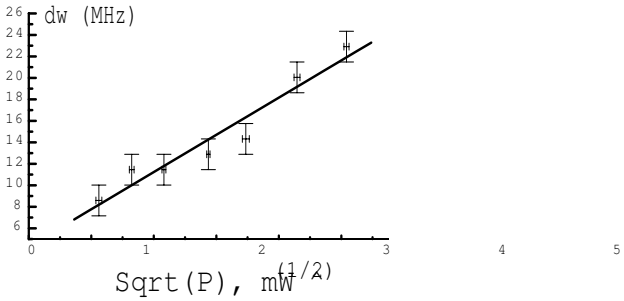

FIG. 20: This shows the splitting between the peaks of signals such as that shown in Fig. 19 vs. Rabi frequency of the $\lambda = 389$ nm light.

VI. CONFERENCE PRESENTATIONS DURING THE GRANT PERIOD

T. Bergeman, "Modeling Alkali Diatomic Energy Levels to Optimize Routes to Ultracold Molecules," (Invited talk) Conference Program, p. 107, Abstract LWD3; Frontiers in Optics 2005/Laser Science XXI; Tuscon, AZ October 16-20, 2005.

Peng Qi, Jianmei Bai, Omer Salihoglu, A. M. Lyyra (Temple U.) and T. H. Bergeman, "Polarization Spectroscopy of Na_2"; B.A.P.S. **51**, No. 3, p. 40: Abstract G1 27, Meeting of the A.P.S. Division of Atomic, Molecular, and Optical Physics (DAMOP) in Knoxville, TN, May 16-20, 2006.

T. H. Bergeman and D. Ananikian, "Damped Oscillations of a BEC in a Double-Well Potential": B.A.P.S. **51**, No. 3, p. 43: Abstract G1 54: Meeting of the A.P.S. D.A.M.O.P. in Knoxville, TN, May 16-20, 2006.

T. H. Bergeman, Y. Huang, H. W. Pechkis, J. Qi, D. Wang, P. L. Gould, E. E. Eyler, W. C. Stwalley, R. A. Cline, J. D. Miller and D. J. Heinzen, "Photoassociation of ^{85}Rb Atoms in 0_u^+ States Near the 5S+5P Atomic Limits," B.A.P.S. **51**, No. 3, p. 72; Abstract L5 2: Meeting of the A.P.S. D.A.M.O.P. in Knoxville, TN, May 16-20, 2006.

X. Miao, E. Wertz, M. G. Cohen and H. Metcalf, "Experimental Progress Toward Multiple Adiabatic Rapid Passage Sequences," B.A.P.S. **51**, No. 3, p. 51: Abstract G1 110: Meeting of the A.P.S. D.A.M.O.P. in Knoxville, TN, May 16-20, 2006.

T. Lu, X. Miao, H. Metcalf, "Nonadiabatic Transitions in Adiabatic Rapid Passage," B.A.P.S. **51**, No. 3, p. 51: Abstract G1 111: Meeting of the A.P.S. D.A.M.O.P. in Knoxville, TN, May 16-20, 2006.

R. Schiller, A. Vernaleken, M. G. Cohen and H. Metcalf, "An Interferometric Technique for the Measurement of Acoustic Velocity," B. A.P.S. **51**, No. 3, p. 106: Abstract O1 125: Meeting of the A.P.S. D.A.M.O.P. in Knoxville, TN, May 16-20, 2006.

C. V. Shean, J. Reeves, M. Keller, M. Riedmann, H. Metcalf, "Neutral Atom Lithography Using a Bright Metastable Helium Beam," B.A.P.S. **51**, No. 3, p. 137: Abstract W1 12: Meeting of the A.P.S. D.A.M.O.P. in Knoxville, TN, May 16-20, 2006.

S.-H. Lee, K. Choi, J. Kaufman, A. Vernaleken, O. Kritsun and H. Metcalf, "Efficient Rydberg Excitation of He with STIRAP", B.A.P.S. **51**, No. 3, p. 154; Abstract W1 115: Meeting of the A.P.S. D.A.M.O.P. in Knoxville, TN, May 16-20, 2006.

S.-H. Lee, K. Choi, J. Kaufman, A. Vernaleken, O. Kritsun and H. Metcalf, "Autler-TownesEffect in Rydberg Excitation of Metastable He Atoms," B.A.P.s. **51**, No. 3, p. 154, Abstract W1 116: Meeting of the A.P.S. D.A.M.O.P. in Knoxville, TN, May 16-20, 2006.

VII. TALKS AT OTHER INSTITUTIONS DURING THE GRANT PERIOD

H. Metcalf, Lectures at TRIUMF, University of British Columbia, July 11-15, 2005:
"Magnetic Trapping of Neutral Atoms," July 11.
"Optical Traps and Optical Lattices," July 12.
"Motion of Meutral Atoms in Traps, Classical and Quantum" July 13.
"Magneto Optical Traps for Neutral Atoms," July 14.
"Bichromatic Optical Forces," July 15.

H. Metcalf, "Optical Forces in Polychromatic Light," Universität Hannover, Germany, Dec. 21, 2005.

H. Metcalf, "Strong Optical Forces in Non-Monochromatic Light", Kansas State University, Nov. 1, 2005; Also at Miami University of Ohio, Nov. 2, 2005; and at Ohio State University, Nov. 4, 2005.

T. Bergeman, "Strategies for Constructing Quantum Computers with Cold Atoms or Polar Molecules": Talk at the Physics Department, United States Military Academy, West Point, Nov. 16, 2005.

T. Bergeman, "From Cold Atoms to Cold Molecules to (Maybe Eventually) a Quantum Computer": Talk

at the Physics Department, Temple University, Jan. 30, 2006.

T. Bergeman, "A Few Comments on Damping of Bose Condensate Excitations": Talk at the University of Heidelberg, Germany: March 9, 2006.

T. Bergeman, "Attempting What is Sometimes Impossible: Fitting Diatomic Potentials and Spin-Orbit Functions to Fragmentary Spectroscopic Data": Talks given at Université Lyon I, Lyon France, March 13, 2006; and at Laboratoire Aimé Cotton, Orsay, France, March 14, 2006.

VIII. MANUSCRIPTS SUBMITTED DURING THE GRANT PERIOD

T. H. Bergeman, Y. Huang, H. W. Pechkis, J. Qi, D. Wang, P. L. Gould, E. E. Eyler, W. C. Stwalley, R. A. Cline, J. D. Miller and D. J. Heinzen, "Photoassociation of ^{85}Rb Atoms in 0_u^+ States Near the 5S+5P Atomic Limits," Accepted for publication in the Journal of Physics B for the special issue on cold molecules, scheduled for September, 2006.

IX. DEMOGRAPHIC DATA FOR THE GRANT PERIOD

a. Number of Scientists Supported: 0.15 faculty and 0.9 grad students.

b. Number of inventions: 0.

c. Number of Ph. D.s awarded: 1. S.-H. Lee, May 25, 2006 (Advisor: H. Metcalf); Xiyue Miao will defend her Ph.D. Thesis work with Prof. Metcalf in August, 2006; David Ananikian will defend his Ph. D. Thesis work with Prof. T. Bergeman also in August, 2006.

d. Number of Bacheler Degrees awareded as a result of this agreement: 0.

e. Number of Patents Submitted: 0.

f. Number of Patents Awareded: 0.

g. Number of Grad Students Supported by this agreement: 1.

h. Number of FTE grad student supported by this agreement: 0.9

i. Number of Post Doctorates supported by this agreement: 0.

j. Number of FRE Post Doctorates supported by this agreement: 0.

k. Number of Faculty supported by this agreement: 0.15.

l. Number of other staff supported by this agreeent: 0.

m. Number of undergrads supported by this agreement: 0.

n. Number of Master Degrees awarded as a result of this agreement: 1; Matthias Riedmann, August, 2005. In addition, Andreas Vernaleken and M. Keller will receive M.S. degrees in August 2006, all based on work with Prof. Metcalf.

X. REPORT OF INVENTIONS

None

[1] M. Cashen and H. Metcalf, J. Opt. Soc. Am. B **20**, 915 (2003).
[2] M. Partlow, X. Miao, J. Bochmann, M. Cashen, and H. Metcalf, Phys. Rev. Lett. **93**, 213004 (2004).
[3] M. Cashen and H. Metcalf, Phys. Rev. A **63**, 025406 (2001).
[4] M. Cashen, O. Rivoire, L. Yatsenko, and H. Metcalf, J. Opt. B: Quant. Semiclass. **4**, 75 (2002).
[5] U. Gaubatz, P. Rudecki, M. Becker, S. Schiemann, M. Kulz, and K. Bergmann, Chem. Phys. Lett. **149**, 463 (1988).
[6] U. Gaubatz, P. Rudecki, S. Schiemann, and K. Bergmann, J. Chem. Phys. **92**, 5363 (1990).
[7] H. L. Bethlem, F. M. H. Crompvoets, R. T. Jongma, S. Y. V. van de Meerakker, and G. Meijer, Phys. Rev. A **65**, 053416 (2002).
[8] T. Bergeman, A. J. Kerman, J. M. Sage, S. Sainis, and D. DeMille, Eur. Phys. J. D **31**, 179 (2004).
[9] J. M. Sage, S. Sainis, T. Bergeman, and D. DeMille, Phys. Rev. Lett. **94**, 203001 (2005).
[10] A. N. Nikolov, E. E. Eyler, X. T. Wang, J. Li, H. Wang, W. C. Stwalley, and P. L. Gould, Phys. Rev. Lett. **82**, 703 (1999).
[11] Y. Huang, Ph.D. thesis, University of Connecticut (2006).
[12] R. A. Cline, J. D. Miller, and D. J. Heinzen, Phys. Rev. Lett. **73**, 632 (1994).
[13] T. Bergeman, J. Qi, D. Wang, Y. Huang, H. K. Pechkis, E. E. Eyler, P. L. Gould, W. C. Stwalley, R. A. Cline, J. D. Miller, et al., J. Phys. B (2006), accepted for publication in the September, 2006 issue.
[14] D. Edvardsson, S. Lunell, and C. M. Marian, Mol. Phys. **101**, 2381 (2003).
[15] M. R. Manaa, A. J. Ross, F. Martin, P. Crozet, A. M. Lyyra, L. Li, C. Amiot, and T. Bergeman, J. Chem. Phys. **117**, 11208 (2002).
[16] R. F. Gutterres, C. Amiot, A. Fioretti, C. Gabbanini, M. Mazzoni, and O. Dulieu, Phys. Rev. A **66**, 024502 (2002).
[17] T. Bergeman, A. Ross, C. Effantin, P. Zalicki, J. Vigué, G. Chawla, R. W. Field, T.-J. Whang, W. C. Stwalley, L. Li, et al., Bull. Amer. Phys. Soc. **49, No. 3**, 74 (2004).
[18] P. Qi, J. Bai, O. Salihoglu, A. M. Lyyra, and T. H. Bergeman, Bull. Amer. Phys. Soc. **51, No. 3**, 40 (2006).
[19] T. Bergeman, P. S. Julienne, C. J. Williams, E. Tiesinga, M. R. Manaa, H. Wang, P. L. Gould, and W. C. Stwalley, J. Chem. Phys. **117**, 7491 (2002).
[20] S. Lee, C. J. Williams, and K. F. Freed, Israel J. Chem. **30**, 3 to 11 (1990).
[21] D. Comparat, C. Drag, B. L. Tolra, A. F. andP. Pillet, A. Cr7ubellier, O. Dulieu, and F. Masnou-Seeuws, Eur. Phys. J. D **11**, 59 (2000).
[22] D. Ananikian and T. Bergeman, Phys. Rev. A **73**, 013604 (2006).
[23] M. Albiez, R. Gati, J. Folling, S. Hunsmann, M. Christiani, and M. K. Oberthaler, Phys. Rev. Lett. **95**, 010402 (2005).
[24] S. Raghavan, A. Smerzi, S. Fantoni, and S. R. Shenoy, Phys. Rev. A **59**, 620 (1999).
[25] G. J. Milburn, J. Corney, E. M. Wright, and D. F. Walls, Phys. Rev. A **55**, 4318 (1997).
[26] T. Lu, X. Miao, and H. Metcalf, Phys. Rev. A **71**, R061405 (2005).
[27] D. Townsend, A. Goodgame, S. Proctor, S. Mackenzie, and T. Softley, J. Phys. B **34**, 439 (2001).
[28] T. Breeden and H. Metcalf, Phys. Rev. Lett. **47**, 1726 (1981).
[29] S. Autler and C. Townes, Phys. Rev. **100**, 703 (1955).